Geophysical Research Letters

RESEARCH LETTER
10.1029/2025GL120291

Robust Yet Diverse Tropical Responses to Antarctic Meltwater Across Models

Xiyue Zhang[1], **Ariaan Purich**[2], **Clara Deser**[3], **and Andrew Pauling**[4,5]

[1]Department of Physics, University of Nevada, Reno, NV, USA, [2]School of Earth, Atmosphere and Environment, and ARC Special Research Initiative for Securing Antarctica's Environmental Future, Monash University, Clayton, VIC, Australia, [3]National Center for Atmospheric Research, Boulder, CO, USA, [4]Department of Physics, University of Otago, Dunedin, New Zealand, [5]Antarctic Research Centre, Victoria University of Wellington, Wellington, New Zealand

Abstract Continued melting of Antarctic ice sheets and shelves adds freshwater to the Southern Ocean (SO), enhancing stratification and inducing surface cooling. This cooling influences tropical climate through coupled atmosphere–ocean interactions, though model responses vary. Using coordinated coupled model experiments with idealized Antarctic meltwater forcing, we assess the remote impacts of SO surface cooling. All 11 models simulate equatorial surface cooling and a northward Intertropical Convergence Zone shift, but show discrepant responses in the equatorial Pacific zonal temperature gradient and Atlantic meridional dipole. When normalized by SO cooling amplitude, these tropical metrics are positively correlated with shortwave cloud feedback strength. Surface energy budget analysis indicates that the previously proposed teleconnection mechanisms in the eastern Pacific are not robust across models. The timescale of tropical cooling and the relative roles of wind-driven latent heat and shortwave fluxes differ across models and basins, highlighting the uncertainty in SO–tropics teleconnections.

Plain Language Summary Melting of Antarctic ice sheets and ice shelves adds freshwater to the Southern Ocean, causing the surface ocean to become more stratified and cooler. Earlier studies suggest that this Southern Ocean cooling can influence tropical climates through air-sea interactions in the eastern Pacific. However, current climate models do not include interactive ice sheets and therefore miss this meltwater effect. In this study, we analyze results from 11 climate models with imposed Antarctic meltwater to test how consistently they simulate these remote impacts. All models show cooling that extends into the tropics, but they differ in how strong this cooling is and where it occurs. By examining the surface energy balance, we find that the processes linking the Southern Ocean to the tropics vary among models and between the Pacific and Atlantic Oceans. These differences challenge the previously proposed pathway via the eastern Pacific, highlighting the need for better understanding of how Antarctic meltwater and Southern Ocean surface cooling influence global climate.

Key Points:

- Coupled models robustly simulate tropical cooling and a northward ITCZ shift in response to Antarctic meltwater input but vary in magnitude
- Models with stronger subtropical low cloud feedbacks tend to show a larger tropical-to-Southern Ocean cooling ratio
- Surface energy budget analysis suggests model-dependent and basin-dependent teleconnection pathways and timescales

Supporting Information:

Supporting Information may be found in the online version of this article.

Correspondence to:

X. Zhang,
xiyuez@unr.edu

Citation:

Zhang, X., Purich, A., Deser, C., & Pauling, A. (2026). Robust yet diverse tropical responses to Antarctic meltwater across models. *Geophysical Research Letters*, *53*, e2025GL120291. https://doi.org/10.1029/2025GL120291

Received 29 OCT 2025
Accepted 27 FEB 2026

Author Contributions:

Conceptualization: Xiyue Zhang, Ariaan Purich, Clara Deser
Data curation: Ariaan Purich, Andrew Pauling
Formal analysis: Xiyue Zhang, Ariaan Purich
Investigation: Xiyue Zhang, Ariaan Purich, Clara Deser
Methodology: Xiyue Zhang, Ariaan Purich, Clara Deser
Project administration: Xiyue Zhang
Software: Xiyue Zhang
Visualization: Xiyue Zhang
Writing – original draft: Xiyue Zhang
Writing – review & editing: Xiyue Zhang, Ariaan Purich, Clara Deser, Andrew Pauling

1. Introduction

It is well established that extratropical forcing can impact tropical climate via coupled atmosphere-ocean processes (Kang et al., 2019; Liu & Alexander, 2007; Seo et al., 2014). While recent Southern Ocean (SO) warming and abrupt Antarctic sea ice decline has been the focus of much attention (Abram et al., 2025; Purich & Doddridge, 2023), these changes contrast the longer term SO surface cooling that has been observed since the start of regular satellite observations (Zhang & Deser, 2024; Zhang et al., 2021). Observed concurrent cooling in the tropical eastern Pacific over recent decades (Wills et al., 2022) has spurred renewed interest in the SO to tropical Pacific teleconnection pathway (Dong, Armour, et al., 2022; Hwang et al., 2017; Kang et al., 2023; Kim et al., 2022; Zhang & Deser, 2024; Zhang et al., 2021). The eastern Pacific cooling has enhanced the zonal sea surface temperature (SST) gradient across the basin, contributing to what is often referred to as the "pattern effect"—a phenomenon linking spatial variations in warming magnitude to climate sensitivity (Rugenstein et al., 2023; Stevens et al., 2016). Recent studies suggest that teleconnections originating from the Southern Ocean can influence observed tropical Pacific SST trends (Dong et al., 2025; Kang et al., 2023; Zhang & Deser, 2024), underscoring the SO's role in modulating global climate feedbacks. Understanding the pattern effect and improving confidence in future climate projections thus requires improved understanding of the drivers behind SO SST trends and the mechanisms by which high-latitude changes influence the tropics.

Previous studies based on various experimental protocols have shown that Southern Ocean cooling induces surface cooling over the tropical southeast Pacific and South Atlantic, as well as a northward shift of the inter-tropical convergence zone (ITCZ; Kang et al., 2019; Kim et al., 2022). This Southern Ocean teleconnection pathway was hypothesized to initiate from climatological northward advection of the Southern Ocean SST anomalies into the subtropical southeast Pacific. There, the shortwave low-cloud feedback, wind-evaporation-surface temperature feedback, and coastal upwelling amplify the local surface temperature anomalies. The anomalies may either remain in the subtropical regions or penetrate into the equatorial Pacific where the Bjerknes feedback further intensifies the cooling (Kim et al., 2022). Questions remain whether this teleconnection pathway operates across different coupled climate models, and if the same pathway exists in the tropical South Atlantic.

Several factors may contribute to the recent cooling of the SO, although models generally fail to reproduce the observed magnitude (Wills et al., 2022). The SO mean-state circulation—characterized by upwelling of deep, relatively unaltered waters—limits surface warming under anthropogenic climate change compared to other regions (Armour et al., 2016). In addition, several mechanisms have been proposed to explain the observed SO cooling during the satellite era, which coincided with an increase in Antarctic sea ice extent until around 2014 (e.g., Dong et al., 2025; Fan et al., 2014; Purich, Cai, et al., 2016; Purich, England, et al., 2016). Accelerating Antarctic meltwater input has emerged as a potential driver of SO surface cooling (Dong, Pauling, et al., 2022; Kaufman et al., 2025; Roach et al., 2023; Rye et al., 2020). Freshwater influx enhances stratification, suppressing vertical mixing and entrainment of warmer subsurface waters, thereby promoting surface cooling (e.g., de Lavergne et al., 2014; Morrison et al., 2015; Purich et al., 2018). Importantly, coupled climate models participating in CMIP6 do not incorporate dynamic ice sheets and shelves (Eyring et al., 2016; Swart et al., 2023) and thus omit the meltwater-induced cooling effect. This omission leads to uncertainty in climate projections (Bronselaer et al., 2018; Fyke et al., 2018; Golledge et al., 2019; Sadai et al., 2020) and may contribute to the models' inability to reproduce observed SO SST trends.

The climatic influence of Antarctic meltwater has been widely studied (e.g., see Table 1 in Swart et al. (2023)), but differences in model configurations and experimental designs have hindered cross-study comparisons. To address this, the Southern Ocean Freshwater Input from Antarctica (SOFIA) Initiative introduced a standardized meltwater forcing protocol, enabling consistent assessment of meltwater impacts across an ensemble of coupled models (Swart et al., 2023). In this study, we leverage the SOFIA ensemble to investigate the pathways through which SO meltwater-induced cooling affects the tropical Pacific and Atlantic Oceans.

Here, we find that the SOFIA multimodel mean reveals cooling in both the eastern tropical Pacific and equatorial Atlantic, in response to Antarctic meltwater additions. Across the ensemble, variations in the magnitude of SO cooling are linked to changes in the Pacific zonal SST gradient and the Atlantic meridional SST dipole. These responses are modulated by the strength of shortwave cloud feedback across models, highlighting this feedback as a key process governing high-latitude to tropical teleconnections.

2. Data and Methods

A detailed description of the SOFIA protocol and simulations can be found in Swart et al. (2023). Briefly, we make use of output from the idealized *antwater* experiment, which is branched off the CMIP6 *piControl* simulation. A freshwater flux anomaly of 0.1 Sv is applied at the surface in Antarctic-adjacent ocean grid cells. This freshwater flux is about 10 times the estimated historical freshwater flux anomaly by 2020, and about a half of the projected basal melt input by 2010 in the high-end emission scenario (ssp585, Figure A1 from Swart et al. (2023)). All other forcings are the same as in *piControl*. The antwater simulations are 100 years long. We define the response to Antarctic meltwater input as the annual mean anomalies of antwater simulations, which are calculated as the difference between the *antwater* average from year 51 to 100 and the *piControl* average of 100 years.

We show results from 11 coupled climate models: ACCESS-ESM1-5 (Ziehn et al., 2020), AWI-ESM-1-RECOM (Semmler et al., 2020), CanESM5 (Swart et al., 2019), CESM2 (Danabasoglu et al., 2020), EC-Earth3 (Döscher et al., 2022), FOCI (Matthes et al., 2020), GFDL-CM4 (Held et al., 2019), GFDL-ESM4 (Dunne et al., 2020), GISS-E2-1-G (Kelley et al., 2020), HadGEM3-GC3.1-LL (Kuhlbrodt et al., 2018), and NorESM2-MM (Seland et al., 2020). The first ensemble member from every model is used for the model inter-comparison (Figures 1–3). The model outputs were regridded onto a common 1° horizontal grid. For the surface energy budget, we analyze outputs from CESM2 and ACCESS-ESM1-5, as the needed variables are not available from other models. These two models each have a small ensemble branched from different years of the *piControl* simulations: three

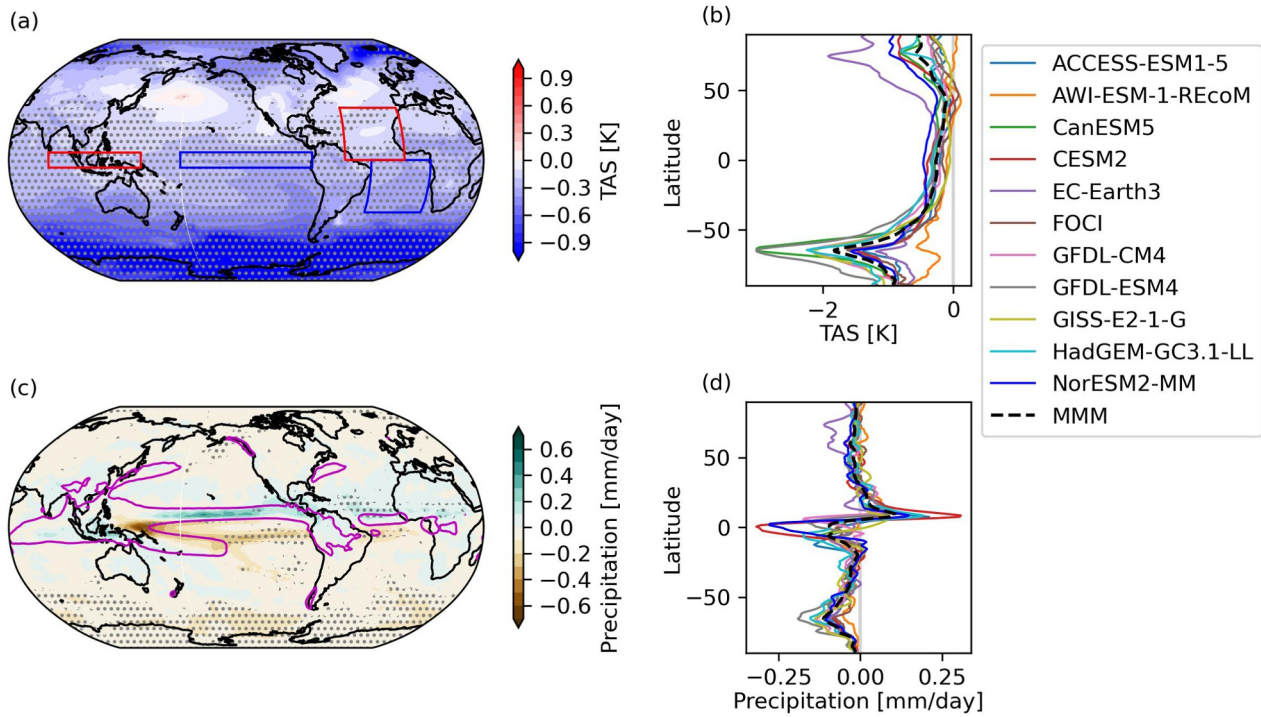

Figure 1. Response of near-surface air temperature (TAS) and precipitation (PR) to *antwater* forcing. (a) Multi-model mean (MMM) TAS response. (b) Zonal-mean TAS response from individual models and MMM. (c) MMM PR response. Magenta contours indicate the MMM *piControl* precipitation of 5 mm/day. (d) Zonal-mean PR response from individual models and MMM. Stippling on the maps indicates agreement in the sign of the response among at least 10 out of 11 models. Red and blue boxes in panel (a) are regions used to calculate metrics in Figure 3.

members for CESM2 and five members for ACCESS-ESM1-5. We use the ensemble mean (CESM-EM and ACCESS-EM) for the surface energy budget analysis to reduce the noise from internal variability on the tropical response (Figure 4).

We perform an energy budget analysis of the mixed layer ocean to provide insight into the physical mechanisms of the SO to tropical teleconnection, following Xie et al. (2010) and Kang et al. (2023). The surface energy balance is given by $\rho C_p H \frac{\partial T}{\partial t} = \mathrm{SW} + \mathrm{LW} - \mathrm{LH} - \mathrm{SH} + O$. The left-hand side represents heat storage: ρ is ocean density, C_p is the specific heat of water, and H is the mixed-layer depth, and T is the mixed-layer temperature (taken as the surface temperature). The right-hand side includes the shortwave flux (SW), longwave flux

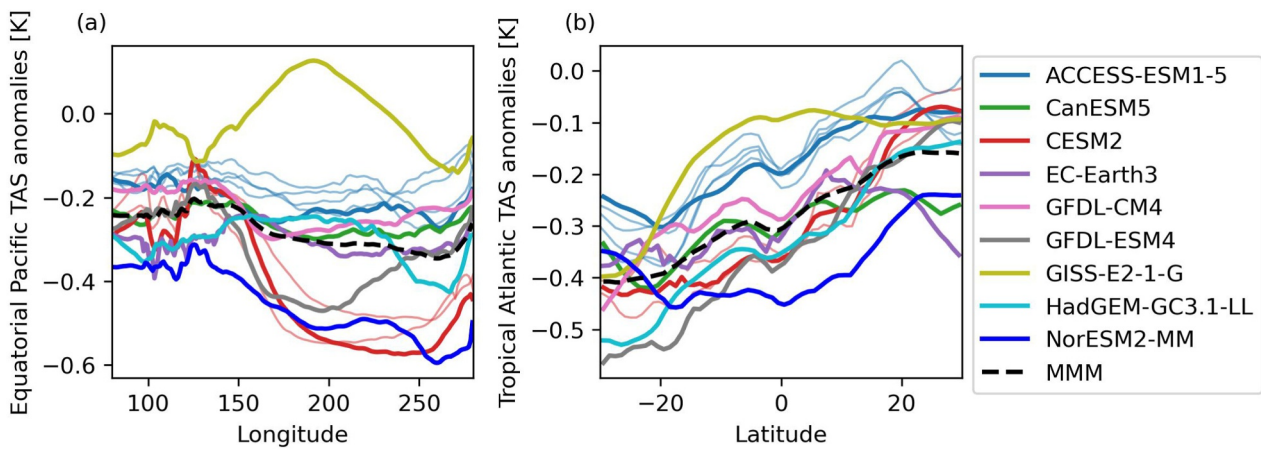

Figure 2. Tropical Pacific and Atlantic TAS responses. (a) Equatorial Pacific (5°S–5°N) average as a function of longitude. (b) Tropical Atlantic (60°W–0°) average as a function of latitude. Light thin lines show additional ensemble members from ACCESS-ESM1-5 and CESM2.

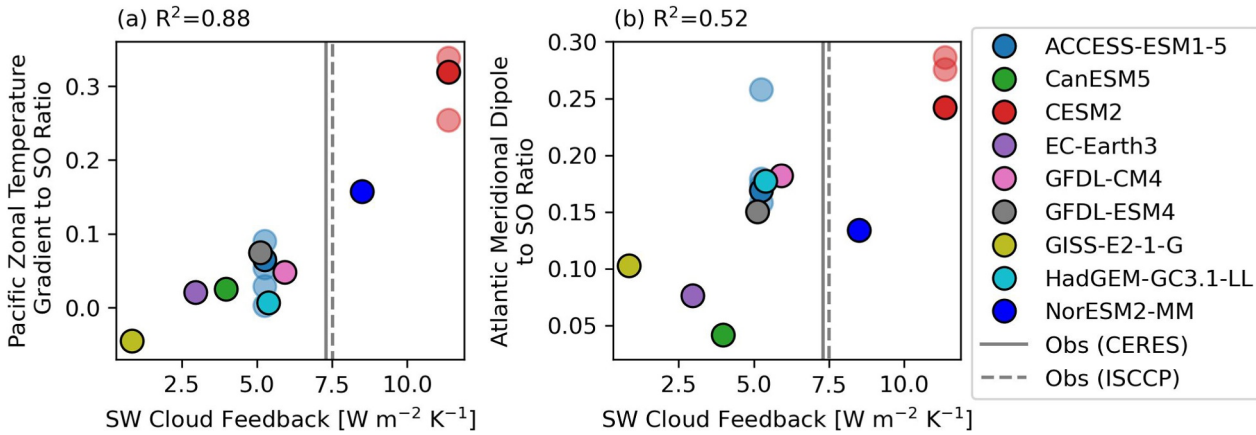

Figure 3. Response ratio of (a) Equatorial Pacific zonal temperature gradient (Figure 1a red box minus blue box in the Pacific) and (b) Atlantic meridional dipole (Figure 1a red box minus blue box in Atlantic) to Southern Ocean temperature, as a function of shortwave cloud feedback strength in the subtropical southeast Pacific. Individual ensemble members from ACCESS-ESM1-5 and CESM2 are shown in lighter shaded circles without black outlines. Correlations (R^2) are calculated using the first ensemble member of each model.

(LW), latent heat flux (LH), sensible heat flux (SH), and ocean dynamics (O). At quasi-equilibrium, the heat storage anomaly is close to zero, so that the ocean dynamics anomaly is calculated as a residual. In a transient state, the heat storage is not negligible but small compared to other terms (Figure 4). Therefore, the ocean dynamics term largely represents the effect of horizontal advection and upwelling/downwelling.

By linearizing the bulk aerodynamic formula for latent heat flux, we can rewrite and diagnose the mixed-layer temperature anomaly ΔT as: $\Delta T = \frac{1}{\alpha \overline{\mathrm{LH}}}(\Delta \mathrm{SW} + \Delta \mathrm{LW} - \Delta \mathrm{SH} + \Delta \mathrm{O} - \Delta \mathrm{LH}_{\mathrm{others}})$, where Δ denotes the response (e.g., *antwater* minus *piControl*), overbar denotes the *piControl* mean, $\alpha = \frac{L_v}{R_v \overline{T}^2} \approx 0.06\ \mathrm{K}^{-1}$ where L_v is the latent heat of vaporization and R_v is the gas constant of moist air. The term $\Delta \mathrm{LH}_{\mathrm{others}} = \Delta \mathrm{LH} - \alpha \overline{\mathrm{LH}} \Delta T$ represents the combined effects of wind speed, relative humidity, and air-sea temperature difference on latent heat flux. Previous studies have shown that wind speed changes often dominate the latent heat flux in the tropical and subtropical oceans (Kang et al., 2023; Zhang et al., 2021). We diagnose the surface temperature anomalies from all terms on the right-hand side for each year and show them in terms of cumulative anoamlies (e.g., values at Year 10 are the difference between the averages of Year 1–10 in *antwater* and 100 years of *piControl*).

3. Results

The multi-model mean (MMM) near-surface air temperature (TAS) shows robust SO cooling in response to Antarctic meltwater forcing (Figure 1a) as expected, given that the meltwater forcing is added to the surface around the Antarctic coast (Swart et al., 2023). Nearly all 11 models show a surface cooling response throughout the Southern Hemisphere, with the cooling gradually weakening toward the equator. The South Pacific shows a prominent zonal asymmetry in its TAS response, where the cooling is strongest in the southeastern portion of the basin and weakest around the Maritime Continent. In the North Pacific, weak warming is evident in the west with cooling in the east, a pattern reminiscent of the negative phase of Pacific Decadal Variability (Mantua et al., 1997), although this response is not present in all models (stippling on Figure 1a, also see Figure S1 in Supporting Information S1). In the Atlantic, cooling gradually weakens northward from the Southern Ocean up to around 40°N. The region of positive TAS anomaly aligns with the location of the North Atlantic "warming hole," a region of reduced warming identified in coupled climate models in response to greenhouse gas forcing. The Arctic shows amplified cooling compared to lower latitudes, a robust response across most models.

While models show agreement on the sign of the TAS response to meltwater input, there is large spread in the magnitude of their responses. In the zonal-mean, the largest spread in TAS response is found over the SO (Figure 1b). While nearly all models display the strongest cooling at around 65°S, the magnitude varies between −3K and −1.4K, which is likely due to different model response in Southern Ocean deep convection (Chen et al., 2023). Interestingly, models with the strongest SO cooling, namely CanESM5 and GFDL-ESM4, do not have the strongest tropical cooling. For example, NorESM2-MM simulates the strongest equatorial cooling of all

the models (−0.45K), yet its SO cooling of −1.6K is weaker than the MMM cooling of −1.8K. In the Arctic, the TAS cooling is slightly amplified, ranging from −3.0 to −0.2K across models. This model spread is indicative of a range of SO teleconnection strength across models.

Accompanying the TAS response, the precipitation response shows unanimous drying over the SO that extends into the Southern Hemisphere subtropics (Figure 1c). The dipole precipitation response in the tropical Pacific is consistent with a northward shift of the ITCZ. In the Atlantic, we also find a northward ITCZ shift with a positive precipitation anomaly extending across the Sahel. Models agree on the eastern Pacific drying and tropical Atlantic dipole response (stippling on Figure 1c), but disagree on the signs of the anomaly in the far western tropical Pacific. The northward ITCZ shift is consistent with zonal-mean energetic arguments whereby precipitation shifts away from the cooler Southern Hemisphere (Kang, 2020).

The zonal-mean precipitation response shows the largest inter-model spread in the tropics (Figure 1d), perhaps not surprisingly, given the large variation of climatological precipitation in the tropics across models (not shown). All models show the precipitation anomaly maximum in the Northern Hemisphere, while the precipitation minimum is in either hemisphere depending on the model. The magnitudes of the zonal-mean precipitation extremes also vary greatly across models: CESM2 shows the largest tropical precipitation anomalies of ±0.3 mm/day, more than twice the magnitude of the MMM anomalies.

Next, we focus on the zonal asymmetry of the equatorial Pacific (5°S–5°N) TAS *antwater* response. The tropical Pacific zonal temperature gradient is an indicator of the Walker circulation strength (Watanabe et al., 2024). Previous studies have pointed out that southern extratropical forcing tends to influence the Walker circulation via changing the tropical Pacific zonal temperature gradient, as surface temperature anomalies tend to preferentially propagate along the eastern ocean basin (Kang et al., 2019). The SOFIA MMM TAS response shows a modest strengthening of the equatorial Pacific zonal temperature gradient, with maximum cooling (−0.3K) in the east and minimum cooling (−0.18K) near the Maritime Continent (Figures 1a and 2a). While 10 out of 11 models agree with this general strengthening pattern (stippling on Figure 1a), the magnitude and longitude of maximum cooling varies greatly. For example, the two end members, GISS-E2-1-G and CESM2, have opposing TAS anomalies of 0.13K and −0.57K in the central and eastern Pacific.

In the Atlantic, we focus on the tropical SST dipole across the equator, which is a major driver of North Atlantic hurricane and Sahel rainfall variabilities (Chang et al., 1997; He et al., 2023). All models consistently show a strengthening of the tropical Atlantic meridional temperature gradient, with greater cooling near 30°S (−0.35K) compared to 30°N (−0.14K) in the MMM (Figure 2b). However, there is a substantial inter-model spread in the magnitude of the tropical Atlantic gradient response. For example, GISS-E2-1-G shows strengthened meridional TAS gradient confined to the Southern Hemisphere, and FOCI has the largest cooling near the equator.

To account for the spread in the SO cooling response to the standardized meltwater forcing across the SOFIA ensemble, we normalize both tropical metrics by the SO TAS anomalies (75°S–50°S) to calculate a response ratio (see Figure S2 in Supporting Information S1 for anomalies without normalization). The inter-model spread in both the tropical Pacific zonal temperature gradient and the tropical Atlantic meridional dipole can be largely explained by the strength of the subtropical shortwave cloud feedback (Figure 3). Here the feedback is defined as the regression of shortwave cloud radiative effect anomalies on local surface temperature anomalies, calculated for the west coast of South America (Table S1 in Kim et al. (2022), only 9 out of 11 models are available). CESM2 shows the strongest shortwave cloud feedback, and has the strongest normalized response in both the Pacific and Atlantic. On the other hand, GISS-E2-1-G shows the weakest shortwave cloud feedback and has the weakest normalized response, which is of the opposite sign in the tropical Pacific. The shortwave cloud feedback strength explains 88% of the intermodel spread of Pacific zonal temperature gradient and 52% of the intermodel spread in the tropical Atlantic meridional dipole. All models except for CESM2 and NorESM2-MM underestimate the shortwave cloud feedback strength compared to observationally derived values of around 7.4 W/m^2 (Kim et al., 2022).

We also find a sizable ensemble spread in the tropical response ratios in the two models with multiple ensemble members. In the tropical Pacific, the zonal temperature gradient response ratio shows a spread of approximately 0.1 across individual members for ACCESS-ESM1-5 and CESM2 (Figure 3a), indicating that internal variability can influence the magnitude of the SO teleconnection even when the forcing is strong. ACCESS-ESM1-5 displays a sizable ensemble spread of 0.12 in the tropical Atlantic dipole response ratio (Figure 3b), suggesting the

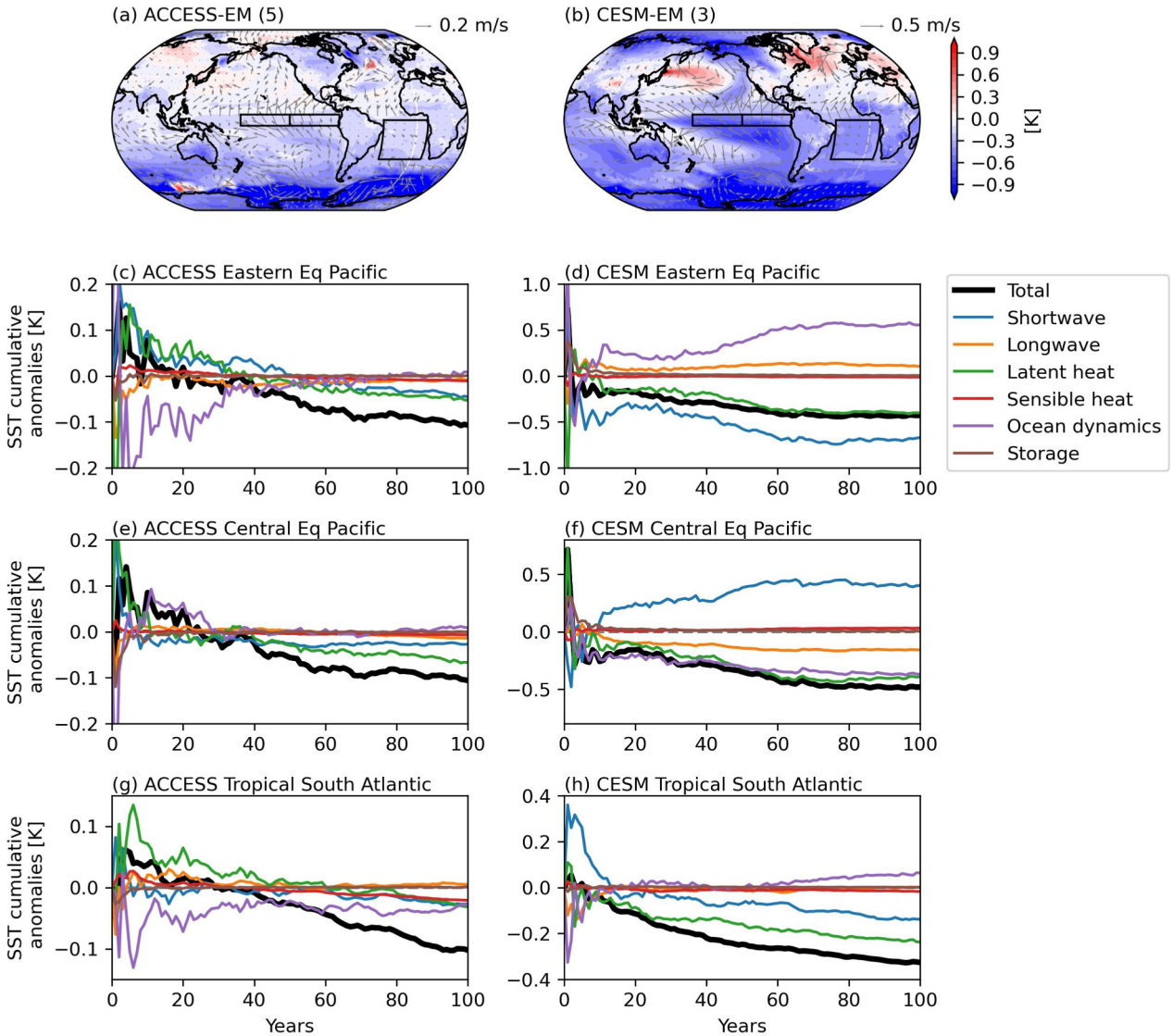

Figure 4. Ensemble mean surface temperature and near-surface wind anomalies from (a) ACCESS-ESM1-5 (five members), and (b) CESM2 (three members). Regional average (outlined by black boxes) of the cumulative timeseries of the terms in the surface energy budget are shown for the eastern equatorial Pacific (130°W–80°W, 5°S–5°N) in panels (c, d), central equatorial Pacific (180°–130°W, 5°S–5°N) in panels (e, f), and tropical south Atlantic (35°W–10°E, 35°S–0°) in panels (g, h).

importance of internal variability, in addition to model uncertainty, in the quasi-equilibrium response to extra-tropical forcing.

To better understand the inter-model spread in the tropical temperature response to Antarctic meltwater forcing, we analyze the surface heat budget of the ocean mixed layer response in the ACCESS-ESM1-5 and CESM2 ensemble means (there is substantial variation in the budget evolution across individual members, see Figures S3 and S4 in Supporting Information S1). We focus on the equatorial Pacific and tropical South Atlantic regions (black boxes in Figures 4a and 4b), as they directly contribute to the equatorial Pacific zonal surface temperature gradient and the tropical Atlantic dipole. We further divide the equatorial Pacific region into a central box (180°–130°W) and an eastern box (130°W–80°W), as the dynamics differ in the two regions. While most surface energy budget analyses focus on the equilibrium response (e.g., Hwang et al., 2017), here we examine the temporal evolution of individual budget terms (Figures 4c–4h).

The equatorial Pacific in ACCESS-ESM1-5 cools by −0.1K at equilibrium (Figures 4c and 4e). Cooling from the latent heat term is consistent with strengthened climatological southeasterlies (Figure 4a), suggesting the role of

wind-evaporation-SST feedback. The shortwave term contributes to cooling more in the eastern than central equatorial Pacific. However, the initial tropical Pacific response shows warming that sustained for nearly two decades. In the eastern Pacific, warming from the latent heat and shortwave terms is counteracted by cooling from ocean dynamics. In the central Pacific, a similar balance only exists in the first 6 years, followed by warming from ocean dynamics.

CESM2 shows a stronger tropical Pacific cooling of about 0.5K at equilibrium (Figures 4d and 4f). The latent heat term contributes to cooling in both the central and eastern Pacific, as the local southeasterly winds strengthens (Figure 4b). However, the shortwave term cools the eastern Pacific but warms the central Pacific, while the ocean dynamics term warms the eastern Pacific but cools the central Pacific. Interestingly, both regions shows warming in the initial years. The eastern Pacific shortwave and latent heat terms switch signs between years 1 and 2, leading to cooling in the region that persists for the rest of the simulation. This demonstrates the importance of the positive shortwave cloud feedback and wind-evaporation-SST feedback in amplifying and prolonging the local cooling in CESM2.

In the tropical South Atlantic, both models show cooling dominated by the latent heat and shortwave terms at equilibrium. However, they have drastically different response timescales. CESM2 shows a gradual cooling driven by the ocean dynamics and longwave terms in the first 10 years (Figure 4g). During this time, the shortwave term remains positive, balancing the cooling. ACCESS-EMS1-5, on the other hand, does not show sustained cooling until year 30 (Figure 4h): initially, there is a balance between the positive latent heat term and the negative ocean dynamics term, but both terms end up contributing to cooling at equilibrium (along with the negative shortwave term). The contrasting initial heat budget response in the two basins highlights potentially different pathways of regional SO teleconnections.

Previous studies have focused on the SO teleconnection pathway in the southeast Pacific. Here, CESM2 shows cooling in the eastern equatorial Pacific by year 3, consistent with Kim et al. (2022) using 22 members of CESM1. ACCESS-ESM1-5 does not show a sustained cooling until Year 20. The shortwave term leads the net cooling in CESM2 by 1 year, suggesting the shortwave cloud feedback's active role, which is not the case in ACCESS-ESM1-5, as the shortwave term remains positive for nearly 50 years. These differences question the robustness of the proposed SO teleconnection mechanism based on a single model.

4. Summary and Discussion

In this study, we make use of an ensemble of 11 coupled climate models running the SOFIA idealized Antarctic meltwater experiment to investigate the remote impact of SO surface cooling. In quasi-equilibrium, all models show widespread cooling extending far beyond the SO, reaching across most ocean basins and over land, except in the western/central North Pacific and subpolar North Atlantic. A northward shift of the ITCZ in the Pacific and Atlantic is found in all models. However, models disagree on the magnitude of the temperature and precipitation responses to consistent meltwater forcing. The responses of the equatorial Pacific zonal temperature gradient and the Atlantic meridional dipole both show large inter-model spread. When normalized to each model's SO response, these two tropical metrics are positively correlated with the shortwave cloud feedback strength. In the low cloud regions, a cooler surface temperature often leads to stronger boundary layer inversion strength and greater low cloud cover (Klein et al., 2017). This reduces the absorbed shortwave radiation at the surface, which further enhances cooling. This local positive feedback allows SO cooling to be enhanced along the west coast of South America, and cooler surface temperatures can further propagate into the lower latitudes via the wind-evaporation-SST feedback (Kim et al., 2022). The surface energy budget sheds light on the distinct evolution of the tropical surface temperature response in the Pacific and Atlantic in two of the models.

Most SO teleconnection studies focus on the Pacific response, as the observed eastern equatorial Pacific cooling remains a challenge for climate models to simulate. Our results confirm earlier studies that the tropical response to SO cooling depends on two key processes: the shortwave cloud feedback and the wind-evaporation-SST feedback (Figures 4c and 4d). Models with stronger subtropical shortwave cloud feedback tend to show a stronger tropical response (Figure 3a). We demonstrate in two models with different shortwave feedback strengths that the timescale of response is also sensitive to the cloud feedback. The stronger-than-observed shortwave cloud feedback in CESM2 allows the eastern equatorial Pacific to quickly cool within the first 3 years, while the weaker-than-observed shortwave cloud feedback in ACCESS-ESM1-5 was not a main driver of the eastern equatorial Pacific cooling. Indeed, it takes nearly 20 years for ACCESS-ESM1-5 to reach a sustained cooling state, largely

from the wind-driven evaporation and shortwave feedbacks. The leading hypothesis of SO teleconnection in the Pacific from Kim et al. (2022) is based on results from a single climate model. Our results show that the proposed mechanism may be highly model dependent, and highlight the value of assessing the teleconnection across multiple models with a common experimental design.

Our study also highlights a potentially different teleconnection pathway in the tropical Atlantic. The tropical Atlantic response to Southern Ocean cooling tends to display a cross-equatorial dipole pattern, with potential implications for Sahel rainfall and hurricane impacts. The stratocumulus cloud deck off the west coast of Africa provides a strong local shortwave cloud feedback, similar to the southeast Pacific (Kim et al., 2022). In CESM2, the shortwave feedback makes a smaller contribution to the tropical south Atlantic cooling than to the eastern Pacific cooling at quasi-equilibrium. In fact, its initial contribution in the tropical Atlantic opposes the cooling. Future work will explore the basin-specific teleconnection pathways in various climate models (e.g., CanESM5, GFDL-CM4 and GFDL-ESM4) in more detail.

Finally, it is important to acknowledge that the real-world Antarctic climate system involves multiple, simultaneously evolving forcings, of which glacial meltwater input is only one component. The multidecade SO surface cooling trend observed since the late 1970s no longer reflects changes observed over the past decade. In particular, recent and ongoing sea ice loss has the potential to enhance Southern Hemisphere surface warming (Abram et al., 2025; Ayres et al., 2022; England et al., 2020), acting in the opposite direction to meltwater-driven surface cooling. Thus, the net Antarctic influence on Southern Ocean surface temperature and far-field tropical responses is more complex than represented in the idealized SOFIA *antwater* meltwater-only experiments. These results therefore highlight the need for coordinated experiments that combine meltwater input with increasing greenhouse gas concentrations (e.g., proposed SOFIA tier 2 historical and SSP experiments), as well as a better process-based understanding of the interplay between meltwater and sea ice, in order to better constrain the remote influence of changes in Antarctica.

Availability Statement

The authors acknowledge the use of various data sets that significantly contributed to this research. The data of the freshwater experiments are available at https://crd-data-donnees-rdc.ec.gc.ca/CCCMA/SOFIA/ (Swart et al., 2023). The CMIP6 *piControl* experiment data (Eyring et al., 2016) are available on the Earth System Grid Federation. Surface energy budget data for ACCESS-ESM1-5 and CESM2 (Zhang, 2026) are available at https://doi.org/10.5281/zenodo.18342793.

Conflict of Interest

The authors declare no conflicts of interest relevant to this study.

Acknowledgments
AP was supported by the Australian Research Council Special Research Initiative for Securing Antarctica's Environmental Future (SR200100005). CD was supported by the National Center for Atmospheric Research (NCAR), which is sponsored by the National Science Foundation under Cooperative Agreement 1852977. Significant effort has been invested by the SOFIA team to design the experiments, the modelers to run the experiments, and by the project members to house the data in an open common archive. Further details are available at https://sofiamip.github.io/ and described in Swart et al. (2023). We specifically thank Torge Martin and Neil Swart for coordinating SOFIA, and those who contributed the antwater experiments used in this study: Ariaan Purich (ACCESS-ESM1-5), Christopher Danek (AWI-ESM-1-REcoM), Neil Swart (CanESM5), Andrew Pauling (CESM2), Eveline van der Linden and Irene Trombini (EC-Earth3), Torge Martin (FOCI), Rebecca Beadling and Stephen Griffies (GFDL-CM4 and GFDL-ESM4), Qian Li (GISS-E2-1-G), Max Thomas (HadGEM3-GC31-LL) and Tore Hattermann (NorESM2-MM) for making their data publicly available, and Neil Swart for processing and documenting antwater output across the model ensemble.

References

Abram, N. J., Purich, A., England, M. H., McCormack, F. S., Strugnell, J. M., Bergstrom, D. M., et al. (2025). Emerging evidence of abrupt changes in the Antarctic environment. *Nature*, *644*(8077), 621–633. https://doi.org/10.1038/s41586-025-09349-5

Armour, K. C., Marshall, J., Scott, J. R., Donohoe, A., & Newsom, E. R. (2016). Southern ocean warming delayed by circumpolar upwelling and equatorward transport. *Nature Geoscience*, *9*(7), 7. https://doi.org/10.1038/ngeo2731

Ayres, H. C., Screen, J. A., Blockley, E. W., & Bracegirdle, T. J. (2022). The coupled atmosphere–ocean response to Antarctic sea ice loss. *Journal of Climate*, *35*(14), 4665–4685. https://doi.org/10.1175/JCLI-D-21-0918.1

Bronselaer, B., Winton, M., Griffies, S. M., Hurlin, W. J., Rodgers, K. B., Sergienko, O. V., et al. (2018). Change in future climate due to Antarctic meltwater. *Nature*, *564*(7734), 53–58. https://doi.org/10.1038/s41586-018-0712-z

Chang, P., Ji, L., & Li, H. (1997). A decadal climate variation in the tropical Atlantic Ocean from thermodynamic air-sea interactions. *Nature*, *385*(6616), 516–518. https://doi.org/10.1038/385516a0

Chen, J.-J., Swart, N. C., Beadling, R., Cheng, X., Hattermann, T., Jüling, A., et al. (2023). Reduced deep convection and bottom water formation due to Antarctic meltwater in a multi-model ensemble. *Geophysical Research Letters*, *50*(24), e2023GL106492. https://doi.org/10.1029/2023GL106492

Danabasoglu, G., Lamarque, J.-F., Bacmeister, J., Bailey, D. A., DuVivier, A. K., Edwards, J., et al. (2020). The Community Earth System Model Version 2 (CESM2). *Journal of Advances in Modeling Earth Systems*, *12*(2), e2019MS001916. https://doi.org/10.1029/2019MS001916

de Lavergne, C., Palter, J. B., Galbraith, E. D., Bernardello, R., & Marinov, I. (2014). Cessation of deep convection in the open Southern Ocean under anthropogenic climate change. *Nature Climate Change*, *4*(4), 278–282. Article 4. https://doi.org/10.1038/nclimate2132

Dong, Y., Armour, K. C., Battisti, D. S., & Blanchard-Wrigglesworth, E. (2022). Two-way teleconnections between the Southern Ocean and the tropical Pacific via a dynamic feedback. *Journal of Climate*, *1*(aop), 1–37. https://doi.org/10.1175/JCLI-D-22-0080.1

Dong, Y., Pauling, A. G., Sadai, S., & Armour, K. C. (2022). Antarctic ice-sheet meltwater reduces transient warming and climate sensitivity through the sea-surface temperature pattern effect. *Geophysical Research Letters*, *49*(24), e2022GL101249. https://doi.org/10.1029/2022GL101249

Dong, Y., Polvani, L. M., Hwang, Y.-T., & England, M. R. (2025). Stratospheric ozone depletion has contributed to the recent tropical La Niña-like cooling pattern. *npj Climate and Atmospheric Science*, *8*(1), 150. https://doi.org/10.1038/s41612-025-01020-0

Döscher, R., Acosta, M., Alessandri, A., Anthoni, P., Arsouze, T., Bergman, T., et al. (2022). The EC-earth3 Earth system model for the coupled model intercomparison project 6. *Geoscientific Model Development*, *15*(7), 2973–3020. https://doi.org/10.5194/gmd-15-2973-2022

Dunne, J. P., Horowitz, L. W., Adcroft, A. J., Ginoux, P., Held, I. M., John, J. G., et al. (2020). The GFDL Earth system model version 4.1 (GFDL-ESM 4.1): Overall coupled model description and simulation characteristics. *Journal of Advances in Modeling Earth Systems*, *12*(11), e2019MS002015. https://doi.org/10.1029/2019MS002015

England, M. R., Polvani, L. M., Sun, L., & Deser, C. (2020). Tropical climate responses to projected Arctic and Antarctic sea-ice loss. *Nature Geoscience*, *13*(4), 1–7. https://doi.org/10.1038/s41561-020-0546-9

Eyring, V., Bony, S., Meehl, G. A., Senior, C. A., Stevens, B., Stouffer, R. J., & Taylor, K. E. (2016). Overview of the Coupled Model Intercomparison Project Phase 6 (CMIP6) experimental design and organization. *Geoscientific Model Development*, *9*(5), 1937–1958. https://doi.org/10.5194/gmd-9-1937-2016

Fan, T., Deser, C., & Schneider, D. P. (2014). Recent Antarctic sea ice trends in the context of Southern Ocean surface climate variations since 1950. *Geophysical Research Letters*, *41*(7), 2419–2426. https://doi.org/10.1002/2014GL059239

Fyke, J., Sergienko, O., Löfverström, M., Price, S., & Lenaerts, J. T. M. (2018). An overview of interactions and feedbacks between ice sheets and the Earth System. *Reviews of Geophysics*, *56*(2), 361–408. https://doi.org/10.1029/2018RG000600

Golledge, N. R., Keller, E. D., Gomez, N., Naughten, K. A., Bernales, J., Trusel, L. D., & Edwards, T. L. (2019). Global environmental consequences of twenty-first-century ice-sheet melt. *Nature*, *566*(7742), 65–72. https://doi.org/10.1038/s41586-019-0889-9

He, C., Clement, A. C., Kramer, S. M., Cane, M. A., Klavans, J. M., Fenske, T. M., & Murphy, L. N. (2023). Tropical Atlantic multidecadal variability is dominated by external forcing. *Nature*, *622*(7983), 521–527. https://doi.org/10.1038/s41586-023-06489-4

Held, I. M., Guo, H., Adcroft, A., Dunne, J. P., Horowitz, L. W., Krasting, J., et al. (2019). Structure and performance of GFDL's CM4.0 climate model. *Journal of Advances in Modeling Earth Systems*, *11*(11), 3691–3727. https://doi.org/10.1029/2019MS001829

Hwang, Y.-T., Xie, S.-P., Deser, C., & Kang, S. M. (2017). Connecting tropical climate change with Southern Ocean heat uptake: Tropical climate change and SO heat uptake. *Geophysical Research Letters*, *44*(18), 9449–9457. https://doi.org/10.1002/2017GL074972

Kang, S. M. (2020). Extratropical influence on the tropical rainfall distribution. *Current Climate Change Reports*, *6*(1), 24–36. https://doi.org/10.1007/s40641-020-00154-y

Kang, S. M., Hawcroft, M., Xiang, B., Hwang, Y.-T., Cazes, G., Codron, F., et al. (2019). ETIN-MIP extratropical-tropical interaction model intercomparison project – Protocol and initial results. *Bulletin of the American Meteorological Society*, *100*(12), 2589–2606. https://doi.org/10.1175/BAMS-D-18-0301.1

Kang, S. M., Yu, Y., Deser, C., Zhang, X., Kang, I.-S., Lee, S.-S., et al. (2023). Global impacts of recent Southern Ocean cooling. *Proceedings of the National Academy of Sciences*, *120*(30), e2300881120. https://doi.org/10.1073/pnas.2300881120

Kaufman, Z., Wilson, E., Purich, A., Beadling, R., & Li, Y. (2025). The impact of underestimated Southern Ocean freshening on simulated historical sea surface temperature trends. *Geophysical Research Letters*, *52*(6), e2024GL112639. https://doi.org/10.1029/2024GL112639

Kelley, M., Schmidt, G. A., Nazarenko, L. S., Bauer, S. E., Ruedy, R., Russell, G. L., et al. (2020). GISS-E2.1: Configurations and climatology. *Journal of Advances in Modeling Earth Systems*, *12*(8), e2019MS002025. https://doi.org/10.1029/2019MS002025

Kim, H., Kang, S. M., Kay, J. E., & Xie, S.-P. (2022). Subtropical clouds key to Southern Ocean teleconnections to the tropical Pacific. *Proceedings of the National Academy of Sciences*, *119*(34), e2200514119. https://doi.org/10.1073/pnas.2200514119

Klein, S. A., Hall, A., Norris, J. R., & Pincus, R. (2017). Low-cloud feedbacks from cloud-controlling factors: A review. *Surveys in Geophysics*, *38*(6), 1307–1329. https://doi.org/10.1007/s10712-017-9433-3

Kuhlbrodt, T., Jones, C. G., Sellar, A., Storkey, D., Blockley, E., Stringer, M., et al. (2018). The low-resolution version of HadGEM3 GC3.1: Development and evaluation for global climate. *Journal of Advances in Modeling Earth Systems*, *10*(11), 2865–2888. https://doi.org/10.1029/2018MS001370

Liu, Z., & Alexander, M. (2007). Atmospheric bridge, oceanic tunnel, and global climatic teleconnections. *Reviews of Geophysics*, *45*(2). https://doi.org/10.1029/2005RG000172

Mantua, N. J., Hare, S. R., Zhang, Y., Wallace, J. M., & Francis, R. C. (1997). A Pacific interdecadal climate oscillation with impacts on salmon production. *Bulletin of the American Meteorological Society*, *78*(6), 1069–1080. https://doi.org/10.1175/1520-0477(1997)078<1069:APICOW>2.0.CO;2

Matthes, K., Biastoch, A., Wahl, S., Harlaß, J., Martin, T., Brücher, T., et al. (2020). The Flexible Ocean and Climate Infrastructure version 1 (FOCI1): Mean state and variability. *Geoscientific Model Development*, *13*(6), 2533–2568. https://doi.org/10.5194/gmd-13-2533-2020

Morrison, A. K., England, M. H., & Hogg, A. M. (2015). Response of Southern Ocean convection and abyssal overturning to surface buoyancy perturbations. *Journal of Climate*, *28*(10), 4263–4278. https://doi.org/10.1175/JCLI-D-14-00110.1

Purich, A., Cai, W., England, M. H., & Cowan, T. (2016). Evidence for link between modelled trends in Antarctic sea ice and underestimated westerly wind changes. *Nature Communications*, *7*(1), 10409. https://doi.org/10.1038/ncomms10409

Purich, A., & Doddridge, E. W. (2023). Record low Antarctic sea ice coverage indicates a new sea ice state. *Communications Earth & Environment*, *4*(1), 314. Article 1. https://doi.org/10.1038/s43247-023-00961-9

Purich, A., England, M. H., Cai, W., Chikamoto, Y., Timmermann, A., Fyfe, J. C., et al. (2016). Tropical Pacific SST drivers of recent Antarctic Sea ice trends. *Journal of Climate*, *29*(24), 8931–8948. https://doi.org/10.1175/JCLI-D-16-0440.1

Purich, A., England, M. H., Cai, W., Sullivan, A., & Durack, P. J. (2018). Impacts of broad-scale surface freshening of the Southern Ocean in a coupled climate model. *Journal of Climate*, *31*(7), 2613–2632. https://doi.org/10.1175/JCLI-D-17-0092.1

Roach, L. A., Mankoff, K. D., Romanou, A., Blanchard-Wrigglesworth, E., Haine, T. W. N., & Schmidt, G. A. (2023). Winds and meltwater together lead to Southern Ocean surface cooling and sea ice expansion. *Geophysical Research Letters*, *50*(24), e2023GL105948. https://doi.org/10.1029/2023GL105948

Rugenstein, M., Zelinka, M., Karnauskas, K., Ceppi, P., & Andrews, T. (2023). Patterns of surface warming matter for climate sensitivity. *Eos*, *104*. https://doi.org/10.1029/2023EO230411

Rye, C. D., Marshall, J., Kelley, M., Russell, G., Nazarenko, L. S., Kostov, Y., et al. (2020). Antarctic glacial melt as a driver of recent Southern Ocean climate trends. *Geophysical Research Letters*, *47*(11), e2019GL086892. https://doi.org/10.1029/2019GL086892

Sadai, S., Condron, A., DeConto, R., & Pollard, D. (2020). Future climate response to Antarctic Ice Sheet melt caused by anthropogenic warming. *Science Advances*, *6*(39), eaaz1169. https://doi.org/10.1126/sciadv.aaz1169

Seland, Ø., Bentsen, M., Olivié, D., Toniazzo, T., Gjermundsen, A., Graff, L. S., et al. (2020). Overview of the Norwegian Earth System Model (NorESM2) and key climate response of CMIP6 DECK, historical, and scenario simulations. *Geoscientific Model Development*, *13*(12), 6165–6200. https://doi.org/10.5194/gmd-13-6165-2020

Semmler, T., Danilov, S., Gierz, P., Goessling, H. F., Hegewald, J., Hinrichs, C., et al. (2020). Simulations for CMIP6 with the AWI climate model AWI-CM-1-1. *Journal of Advances in Modeling Earth Systems*, *12*(9), e2019MS002009. https://doi.org/10.1029/2019MS002009

Seo, J., Kang, S. M., & Frierson, D. M. W. (2014). Sensitivity of intertropical convergence zone movement to the latitudinal position of thermal forcing. *Journal of Climate*, *27*(8), 3035–3042. https://doi.org/10.1175/JCLI-D-13-00691.1

Stevens, B., Sherwood, S. C., Bony, S., & Webb, M. J. (2016). Prospects for narrowing bounds on Earth's equilibrium climate sensitivity. *Earth's Future*, *4*(11), 512–522. https://doi.org/10.1002/2016EF000376

Swart, N. C., Cole, J. N. S., Kharin, V. V., Lazare, M., Scinocca, J. F., Gillett, N. P., et al. (2019). The Canadian Earth System Model version 5 (CanESM5.0.3). *Geoscientific Model Development*, *12*(11), 4823–4873. https://doi.org/10.5194/gmd-12-4823-2019

Swart, N. C., Martin, T., Beadling, R., Chen, J.-J., Danek, C., England, M. H., et al. (2023). The Southern Ocean Freshwater Input from Antarctica (SOFIA) Initiative: Scientific objectives and experimental design. *Geoscientific Model Development*, *16*(24), 7289–7309. https://doi.org/10.5194/gmd-16-7289-2023

Watanabe, M., Kang, S. M., Collins, M., Hwang, Y.-T., McGregor, S., & Stuecker, M. F. (2024). Possible shift in controls of the tropical Pacific surface warming pattern. *Nature*, *630*(8016), 315–324. https://doi.org/10.1038/s41586-024-07452-7

Wills, R. C. J., Dong, Y., Proistosecu, C., Armour, K. C., & Battisti, D. S. (2022). Systematic climate model biases in the large-scale patterns of recent sea-surface temperature and sea-level pressure change. *Geophysical Research Letters*, *49*(17), e2022GL100011. https://doi.org/10.1029/2022GL100011

Xie, S.-P., Deser, C., Vecchi, G. A., Ma, J., Teng, H., & Wittenberg, A. T. (2010). Global warming pattern formation: Sea surface temperature and rainfall. *Journal of Climate*, *23*(4), 966–986. https://doi.org/10.1175/2009JCLI3329.1

Zhang, X. (2026). Surface energy budget dataset for "Robust yet Diverse Tropical Responses to Antarctic Meltwater Across Models" [Dataset]. *Zenodo*. https://doi.org/10.5281/zenodo.18342793

Zhang, X., & Deser, C. (2024). Tropical and Antarctic sea ice impacts of observed Southern Ocean warming and cooling trends since 1949. *npj Climate and Atmospheric Science*, *7*(1), 1–9. https://doi.org/10.1038/s41612-024-00735-w

Zhang, X., Deser, C., & Sun, L. (2021). Is there a tropical response to recent observed Southern Ocean cooling? *Geophysical Research Letters*, *48*(5), e2020GL091235. https://doi.org/10.1029/2020GL091235

Ziehn, T., Chamberlain, M. A., Law, R. M., Lenton, A., Bodman, R. W., Dix, M., et al. (2020). The Australian Earth System model: ACCESS-ESM1.5. *Journal of Southern Hemisphere Earth Systems Science*, *70*(1), 193–214. https://doi.org/10.1071/ES19035